Automatic Segmentation of Renal Compartments in DCE-MRI Images

Xin Yang[1], Hung Le Minh[1], Tim Cheng[2], Kyung Hyun Sung[3], and Wenyu Liu[1]

[1] Huazhong University of Science and Technology, China
[2] University of California, Santa Barbara, USA
[3] University of California, Los Angeles, USA
xinyang2014@hust.edu.cn, leminhhung@hcmutrans.edu.vn,
timcheng@ece.ucsb.edu, ksung@mednet.ucla.edu,
liuwy@mail.hust.edu.cn

Abstract. In this paper, we introduce a method for automatic renal compartment segmentation from Dynamic Contrast-Enhanced MRI (DCE-MRI) images, which is an important problem but existing solutions cannot achieve high accuracy robustly for a wide range of data. The proposed method consists of three main steps. First, the whole kidney is segmented based on the concept of Maximally Stable Temporal Volume (MSTV). The proposed MSTV detects anatomical structures that are stable in both spatial domain and temporal dynamics. MSTV-based kidney segmentation is robust to noises and does not require a training phase. It can well adapt to kidney shape variations caused by renal dysfunction. Second, voxels in the segmented kidney are described by principal components (PCs) to remove temporal redundancy and noises. And then k-means clustering of PCs is applied to separate voxels into cortex, medulla and pelvis. Third, a refinement method is introduced to further remove noises in each segmented compartment. Experimental results on 16 clinical kidney datasets demonstrate that our method reaches a very high level of agreement with manual results and achieves superior performance to three existing baseline methods. The code of the proposed method will be made publicly available with the publication of this paper.

1 Introduction

DCE-MRI has been proved to be the most advantageous imaging modality of the pediatric kidney [1], providing one-stop comprehensive morphological and functional information, without the utilization of ionizing radiation. Accurate segmentation of renal compartments (i.e. cortex, medulla and renal pelvis) from DCE-MRI images is essential for functional kidney evaluation; however, there still lacks of effective and automatic solutions. Several limitations of DCE-MRI images make this task particularly challenging: 1) low spatial resolution, poor signal-to-noise ratio and partial volume effects due to fast and repeated scanning, 2) inhomogeneous intensity changes during perfusion in each compartment, especially for disordered kidneys.

Several papers in the literature tackle the problem of renal compartment segmentation. In [2], authors handled cortex segmentation as a multiple-surface extraction

N. Navab et al. (Eds.): MICCAI 2015, Part I, LNCS 9349, pp. 3–11, 2015.
DOI: 10.1007/978-3-319-24553-9_1

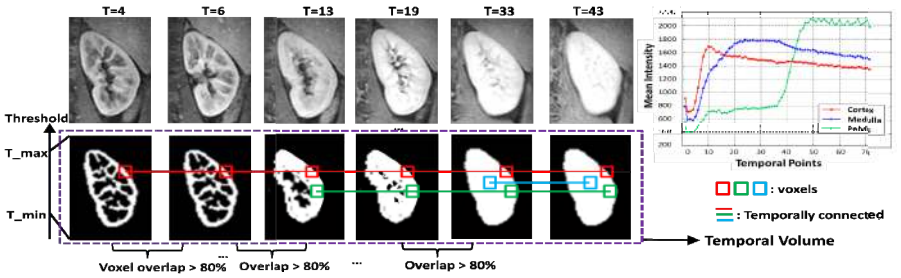

Fig. 1. (1) The top row on the left: a slice of DCE-MRI series taken at 6 temporal points 3, 6, 13, 19, 33 and 43. For this patient, 2448 abdomen images were taken over 72 temporal points. As time increases, the cortex, the medulla and the pelvis are highlighted sequentially. (2) The bottom row on the left: segmentation via thresholding. Red, green and blue rectangles denote voxels at three kidney locations. Voxels connected using solid lines are temporally connected. We define two segmented volumes are temporally connected if they are temporally adjacent and the voxel overlap between them is greater than 80%. A sequence of temporally connected volumes is denoted as a temporal volume (indicated in the purple dashed rectangle). (3) The right figure indicates typical time-intensity curves for compartments of a normal kidney.

problem, which is solved using the optimal surface search method based on a graph construction scheme. This method is primarily designed for 3D CT images and evaluated on CT data, thus valuable temporal information embedded in the intensity time courses of DCE-MRI images is not considered (i.e. the temporal intensity evolution is different for each of the three kidney compartments, as shown in the top row of the left part of Fig. 1 and the chart on the right part of Fig. 1). To address this problem, Sun et al. [3] proposed an energy function that exploits both the spatial correlation among voxels and the intensity change of every voxel across the image sequences. In [4] and [5], the authors employed k-means clustering of temporal intensity evolution to segment the three internal renal structures. However, those methods were evaluated only on normal kidneys; in practice they are sensitive to pathologies. Recently, Khrichenko et al. [1] presented a program, named CHOP-fMRU, for renal compartment segmentation and functional analysis. CHOP-fMRU involves several manual tasks (e.g. manual delineation of a rough kidney contour for initialization) and the quality of the segmentation and analysis results depends heavily on the quality of the manual tasks.

There have been numerous dedicated research efforts [6, 7, 8, 9, 10, 11] for automatic segmentation of whole kidneys. Some of the most popular ones rely on the shape and appearance models learned from a set of previously segmented kidneys. For instance, Spiegel et al. [11] learned the kidney mean shape and principal modes of variation via an Active Shape Model to constrain the segmentation results. Yuksel et al. [10] modeled the kidney shape and intensity distribution using a signed distance map and Gaussian mixture models, respectively. In [8, 9], the authors integrated shape priors into a geometric deformable model to extract the kidney region. Model-based approaches have demonstrated promising results for segmenting an entire healthy kidney. However, the structure of renal compartments is much more challenging to model than a whole kidney due to its high complexity and variability in shape, in particular for those of disordered kidneys. As a result, it's challenging for model-based methods to achieve satisfactory results for dysfunctional kidneys and for inner compartment segmentation.

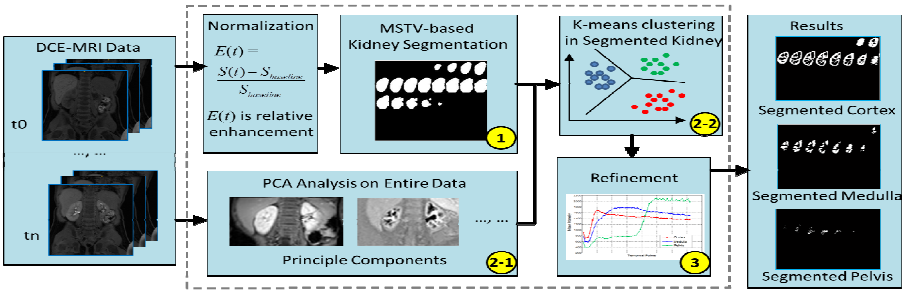

Fig. 2. Illustration of the proposed renal compartment segmentation framework

In this paper, we propose an automatic method which can segment renal compartments for DCE-MRI images from both healthy subjects and patients with kidney problems. The proposed method, which demonstrates excellent agreement with manual segmentation results, consists of three main steps, as illustrated in Fig. 2. First, a whole kidney is automatically segmented from abdominal images based on the detection of *Maximally Stable Temporal Volume* (MSTV). The proposed MSTV exploiting both 3D spatial correlation among voxels and temporal dynamics for each voxel to provide a reliable segmentation robust to noises from surrounding tissues and kidney shape variations. Second, voxels in the segmented kidney are described by N principal components (PCs) where N is an empirical parameter. Our extensive experimental results indicate that for all cases the first 10 PCs capture most information needed for renal compartment segmentation. Thus discarding the rest of the components can effectively remove temporal redundancy and suppress noises with little loss of useful information. K-means clustering of the PCs is then leveraged to cluster voxels into the cortex, the medulla and the pelvis respectively. Third, an effective and fast refinement method is proposed to remove noises in each segmented compartment. The proposed segmentation method has been tested using 16 clinical kidney data and compared with the manual results and the results produced by three baseline methods. The results of the proposed method show excellent agreement with the manual results and superior performance to the baseline methods.

2 Our 3-Step Method

2.1 Step 1 – Initial Segmentation Based on MSTV

As contrast agent perfuses into a kidney, intensity contrast between the kidney and its surrounding tissues are enhanced gradually (as shown in the top row of the left part of Fig. 1). As a result, when binarizing a 3D volume via thresholding after contrast injection, the voxels in the segmented kidney possess three characteristics: 1) they are stable across a wide range of thresholds (as shown in the bottom row of the left part of Fig. 1); 2) most of them are spatially connected (i.e. one voxel is among the other's 26 neighbors of another voxel in the segmented kidney); 3) a large portion of them appear in the temporally adjacent segmented volumes (i.e. having large voxel overlap in their temporal dynamics). In contrast, intensity enhancement of non-kidney tissues is

Pseudo Code 1: MSTV-based Whole Kidney Segmentation from a DCE-MRI series

Input: DCE-MRI data $\boldsymbol{V} = \{V_1, \ldots V_{t-1}, \ldots V_T\}$,
All possible thresholds $\boldsymbol{J} = \{1,\ldots j,\ldots J\}$, j is ranked in an increasing order
Parameters λ , τ and α

Output: Segmentation of a whole kidney

Procedure1: Connected Component Trees Construction

for $V_t = V_1, \ldots V_T$
for $j = 1,\ldots J$
Binarize V_t using threshold j → a list of connected voxels, $\{\ldots (v_t^j)_i \ldots\}$;
Insert $\{\ldots (v_t^j)_i \ldots\}$ → the j^{th} level of Tree Tr_t ;
Insert Tree Tr_t → Connected Component Trees $\boldsymbol{Tr} = \{Tr_1, \ldots Tr_t\}$

Procedure2: Maximum Stable Temporal Volumes Detection

for $j = 1,\ldots J$
Find temporally connected sequence $\vartheta_j^k = \{\ldots, v_{t-1}^j, \ldots\}_k$ $(1 \le k \le K)$
K is the total number of temporal volumes in level j
Transverse $\boldsymbol{Tr}$ from root to the level J to detect M sequences of nested temporal volume $\{\vartheta_1, \ldots, \vartheta_{j-1}, \vartheta_j \ldots\}_m$ $(1 \le m \le M)$
Calculate $S_m(j*)$ for each $\{\vartheta_1, \ldots, \vartheta_{j-1}, \vartheta_j \ldots\}_m$
Search $m*$ which achieves maximum $S_m(j*)$,and sequence is $\{\vartheta_{j*-\beta_{j*}}, \ldots, \vartheta_{j*}\}_{m*}$

Procedure3: MSTV-based Whole Kidney Segmentation

Construct histogram $\boldsymbol{H}$=$\{h_1,\ldots,h_N\}$ for voxels in $\{\vartheta_{j*-\beta_{j*}}, \ldots, \vartheta_{j*}\}_{m*}$, $N = |\vartheta_{j*}|$
for $\vartheta_k = \{\vartheta_{j*-\beta_{j*}}, \ldots, \vartheta_{j*}\}_{m*}$
Update corresponding items of $\boldsymbol{H}$ for voxels appear in ϑ_k
Select voxels whose votes in $\boldsymbol{H}$ is greater than α → whole kidney segmentation

rare and random; therefore, segmented non-kidney voxels are sensitive to thresholds, usually are not spatially connected and have small overlap in temporal domain. Based on the characteristics described above, in the following we describe a concept of *Maximally Stable Temporal Volume* (MSTV) and propose its application to whole kidney segmentation. Formal definitions *Temporal Volume* and MSTV are as follows:

1) **Temporal Volume.** We denote $v_t\ (1 \le t \le T)$ as a set of spatially connected voxels segmented from original 3D volume at temporal point t by thresholding. T is the total number of temporal points in a DCE-MRI series. We define $v_{t-1}, v_t\ (1 \le t - 1 < t \le T)$ are *temporally connected* if v_{t-1}, v_t have greater than λ (λ is 80% in this study) segmented voxels in common (i.e. voxel overlap between them > λ). If a sequence $\vartheta = \{v_1, \ldots, v_{t-1}, v_t\}$ $(t \ge 2)$ that any two temporally consecutive voxel sets in the sequence are *temporally connected*, we denote the sequence ϑ as a temporal volume. The cardinality of ϑ is defined as $|\vartheta| = \sum_1^t |v_i|$

2) **Maximally Stable Temporal Volume.** If ϑ_{j-1}, ϑ_j are two temporal volumes obtained using threshold j-1 and j respectively, and $v_1^{j-1} \subseteq v_1^j, \ldots, v_{t-1}^{j-1} \subseteq v_{t-1}^j$, $v_t^{j-1} \subseteq v_t^j$, then ϑ_{j-1} is a subset of ϑ_j i.e. $\vartheta_{j-1} \subseteq \vartheta_j$. Let $\{\vartheta_1, \ldots, \vartheta_{j-1}, \vartheta_j \ldots\}_m$ $(1 \le m \le M)$

Fig. 3. First 10 PCs of a dynamic DCE-MRI data

be a sequence of nested temporal volumes, M is the total number of nested sequences detected in DCE-MRI data, the stability of the sequence is defined as:

$$S(j) = \beta_j \times |\vartheta_j| \tag{1}$$

Eq.(1) evaluates the stability of a segmentation, where β_j and $|\vartheta_j|$iindicate across how many consecutive thresholds and how many temporally adjacent trees the segmentation could remain stable respectively. We search j^* which provides maximum $S_m(j*)$ for $\{\vartheta_1, \ldots, \vartheta_{j-1}, \vartheta_j \ldots\}_m$. For all M sequences of nested temporal volumes, we select m^* which achieves a maximum $S_{m^*}(j*)$ which implies a combination of both large cardinality of ϑ_{j*} and stability of ϑ_{j*} across a wide range of parameters.

The detection process of MSTV is illustrated in Pseudo Code 1. First, for every volumetric data at time t ($1 \le t \le T$), a *connected component tree* Tr_t is constructed by binarizing the volume v_t using all possible thresholds j's ($1 \le j \le J$,). A node at level j of tree Tr_t consists of a group of spatially connected voxels. Second, for every threshold i (i.e. level j of the trees), we transverse trees $\boldsymbol{Tr} = \{Tr_1, \ldots Tr_T\}$ along temporal axis to search for all temporal volumes. Then we transverse trees $\boldsymbol{Tr}$ vertically from roots to the last level J to detect MSTV. Third, we select voxels which appear in most temporal volumes in MSTV to form initial whole kidney segmentation. A dilation operation is also applied to fill holes inside the kidney segmentation.

Our MSTV can be considered as an extension of *Maximally Stable Extremal Region* (MSER) [13], one of the best interest point detectors in computer vision, from 2D to 4D. Meanwhile, we propose a MSTV detection method based on connected component trees and apply it for kidney segmentation. Our MSTV does not impose any shape constraints on the segmentation results, thus it can adapt to kidney shape variations caused by renal dysfunction.

2.2 Step 2 – PCA-kmeans Clustering for Renal Compartment Segmentation

Time intensity curves associated with the cortex, the medulla and the pelvis voxels are distinguishable from each other (as shown in the right chart of Fig.1). Therefore, they could be separated by unsupervised clustering of time intensity curves. However, the raw temporal data often has a high dimension, which increases the computation cost and induces numerical problems. Moreover, not all voxels of the same tissue are highlighted at the same moment, leading to misalignment of curves which belong to the same tissue and in turn resulting in mis-classification. In addition, most dimensions in the raw temporal data are redundant; the redundancy would dilute the useful information and disturb the true distribution.

To address these problems, we employ Principal Component Analysis (PCA) to reduce the dimension of the temporal data. Voxel features in the temporal dimension are then described by a set of principal components (PCs). PCA transforms the raw

data into a new coordinate space, such that the greatest variance lies along the first coordinate (denoted as 1st PC), the second greatest variance along the second coordinate, and so on. By discarding the less significant components, PCA can reduce the dimension of dynamic data and suppress noises. In addition, by linearly combining several temporal dimensions to form a new feature dimension, misalignment can be avoided. Thorough analysis of our experimental results show that, for all cases we experimented with, greater than 99.4% of the total information is included in the first 10 PCs. As illustrated in Fig. 3, the 1st principal component captures most global information of a kidney, and the 2nd to the 10th components encode detailed information of inner structures. For the later PCs, the variances tend to be more dominantly affected by noise. Based on our experiment study, we choose 10 PCs for further analysis.

Once voxels in the segmented kidney are described by the first 10 PCs, unsupervised clustering is applied to separate voxels into three groups: the cortex, the medulla and the pelvis. Among a number of suitable clustering methods, we choose k-means clustering in this study due to its simplicity, efficiency and effectiveness.

2.3 Step 3 – Refinement

We propose a refinement method for removing noise induced in Step 1 and for recovering mis-classification due to ambiguous boundaries between clusters in the principal component space. The refinement method starts from the segmented cortex, to the medulla and then to the pelvis. First, for each candidate cortex voxel obtained in Step 2 we calculate its *maximum intensity enhancement* (MIE) by subtracting its pre-contrast intensity from its maximum intensity. Based on the fact that cortex voxels are mostly highlighted at similar moments, we compute the average intensity of all cortex voxels at each temporal point and select a point t_{max} whose average intensity reaches the maximum. We consider t_{max} and its neighboring temporal points $t_{max\text{-}1}$ and t_{max+1} as the candidate moments at which the cortex tissues are maximally highlighted. Accordingly, MIE for cortex voxel i is calculated based on Eq. (2):

$$MIE_{cortex}(i) = \max\left\{\left(S_{t_{\max-1}}(i) - S_b(i)\right),\ \left(S_{t_{\max}}(i) - S_b(i)\right),\ \left(S_{t_{\max+1}}(i) - S_b(i)\right)\right\}\quad i \subset \{\text{candidate cortex voxels}\} \tag{2}$$

At $t_{max\text{-}1}$, t_{max} and t_{max+1}, the intensities of medulla and non-kidney tissues do not change too much from their pre-contrast intensities. Thus, at those moments, the MIE of voxels should be much smaller than the cortex voxels and hence can be easily excluded by thresholding. The threshold is automatically selected via the Otsu method [15]. Second, we attempt to recover the mis-detection of true cortex voxels. For every non-cortex voxel within the segmented kidney, we examine its spatially adjacent voxels. If all of them are labeled as cortex voxels after the noise removal step described above, we re-label it from a non-cortex to a cortex voxel. Similarly, this refinement method is also applied to the segmented medulla and pelvis.

3 Experimental Results

This study, approved by the local institutional review board, consists of evaluation of 16 kidney cases: 7 normal cases, 7 disordered cases, and 2 cases with operations where the medulla and the pelvis were removed. The MRI data acquisition was

Table 1. Comparison of Segmentation Methods

	Compartment	Our method	w/o MSTV	w/o PCA	Region Completion
Disordered Kidneys	Cortex	0.86	0.72	0.54	0.59
	Medulla	0.95	0.65	0.51	0.52
	Pelvis	0.69	0.54	0.56	0.60
Kidneys with Op.	Cortex	0.92	0.39	0.47	0.45
Healthy Kidneys	Cortex	0.97	0.74	0.58	0.49
	Medulla	0.98	0.74	0.51	0.52
	Pelvis	0.95	0.79	0.74	0.60

performed using a 3.0T GE MR 750 system. To minimize the risk of gadolinium in patients with impaired kidney function, a low dose at 1/5 of Gadovist was used as the contrast agent with the injection rate of 0.3 mL/s, followed by 10mL saline chaser at the same rate. The DCE-MRI data sets were acquired by ventilator controlled breath-hold and have sufficient temporal alignment in most cases. Bellows respiratory triggering was implemented resulting in a temporal phase every two respiratory cycles. A 3D T1-weighted gradient echo sequence with a dual-echo bipolar readout was used for data acquisition, and we used an in-house variable density Cartesian undersampling scheme called DISCO to perform high spatiotemporal resolution dynamic MRU [14]. A two-point Dixon reconstruction was used for robust fat–water separation. Imaging parameters were: flip angle is 15^o, TR=3.56ms, matrix size=256×256, FOV= 340×340 mm^2, the total number of slices is 34, and slice thickness is 4 mm.

We evaluated the segmentation accuracy using the Dice Similarity Coefficient (DSC), a widely used metric to evaluate segmentation algorithms for different medical image modalities. The DSC is defined as:

$$DSC(S,G) = \frac{2\times|S\cap G|}{|S|+|G|} \tag{3}$$

where S and G represent the sets of automatically segmented voxels and manually segmented voxels respectively; $|\cdot|$ denotes the set cardinality. The DSC ranges from 0, if S and G do not overlap at all, to 1, if S and G are identical.

We compare our method with three baseline methods: Region Competition [12], a popular active contour method for segmentation, our method without MSTV-based kidney segmentation (denoted as w/o MSTV) and our method without PCA dimension reduction (denoted as w/o PCA). We used the implementation in ITK-SNAP for Region Competition. Since Region Competition is originally designed for 2D or 3D, but not 4D, data, we manually selected 3D volumes at those temporal points when the cortex, the parenchyma (i.e. the cortex and the medulla) and a whole kidney respectively seem maximally highlighted. Region Competition is applied to each 3D volume to segment the cortex, the parenchyma and a whole kidney; the medulla and the pelvis were obtained by subtracting the cortex from the segmented parenchyma, and by subtracting the parenchyma from the whole kidney, respectively.

Table 1 summarizes the average DSC for all four methods. Three observations can be made from Table 1. First, the DSC achieved by our method is over 0.9 for most cases except for the cortex (0.86) and the pelvis (0.69) of disordered kidneys. This might be because part of the cortex and pelvis tissues were not highlighted due to the

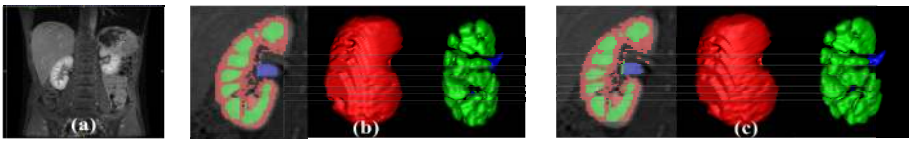

Fig. 4. (a) An exemplar abdominal image from DCE-MRI data. 2D and 3D segmentation of inner compartments based on (b) manual label and (c) our method.

renal disease, causing disconnection among voxels in the spatial and temporal domains. Second, MSTV and PCA dimension reduction are essential and complementary to accurate segmentation results, i.e. 14%~59% and 13%~48% improvements are achieved by using the MSTV-based whole kidney segmentation and by PCA dimension reduction, respectively. Third, the average DSC of our method is 9%~51% higher than those of Region Competition. We believe Region Competition's poor performance is mainly due to the highly varying contrast during perfusion. Although we manually selected the most relevant volumes in different phases of perfusion, it remains challenging to distinguish internal renal structures from a single image sequence. Fig. 4 illustrates an image from a DCE-MRI sequence and the corresponding segmentation results based on manual labeling (b) and our automatic method (c).

4 Conclusion and Future Work

We present a method for automatic renal compartment segmentation from DCE-MRI. The proposed method first segments a whole kidney based on the detection of MSTV. MSTV is a collection of spatially and temporally connected voxels that can be robustly segmented across a wide range of thresholds and temporal dynamics. Voxels in an MSTV well represents characteristics of kidney voxels and hence is applicable to whole kidney segmentation. MSTV-based kidney segmentation is robust to noises and can adapt to kidney shape variations due to renal dysfunction. With a whole kidney segmented, the proposed method clusters the segmented kidney voxels into three groups: the cortex, the medulla and the pelvis, via PCA and k-means clustering. Experimental results show that PCA plays an essential role for high segmentation accuracy. Finally, a refinement method based on maximum intensity enhancement is employed for removing noise and for recovering mis-detected kidney voxels. Our future work includes further acceleration of the current method, further accuracy improvement through renal compartment recognition, and proper motion correction via image registration.

References

1. Khrichenko, D., Darge, K.: Functional Analysis in MR Urography – Made Simple. Pediatr. Radiol. 40, 182–199 (2010)
2. Li, X., Chen, X., Yao, J., Zhang, X., Tian, J.: Renal cortex segmentation using optimal surface search with novel graph construction. In: Fichtinger, G., Martel, A., Peters, T. (eds.) MICCAI 2011, Part III. LNCS, vol. 6893, pp. 387–394. Springer, Heidelberg (2011)

3. Sun, Y., Moura, M.F., Yang, D., Ye, Q., Ho, C.: Kidney Segmentation in MRI Sequences using Temproal Dynamics. In: Proc. of IEEE ISBI, pp. 98–101 (2002)
4. Zollner, F.G., Sance, R., Rogelj, P., Ledesma-Carbayo, M.J., Rorvik, J., Santos, A., Lundervold, A.: Assessment of 3D DCE-MRI of the Kidneys using Non-rigid Image Registration and Segmentation of Voxel Time Courses. Comput. Med. Imag. and Gra., 171–181 (2009)
5. Chevaillier, B., Ponvianne, Y., Collette, J.L., Mandry, D., Claudon, M., Pietquin, O.: Functional Semi-automated Segmentation of Renal DCE-MRI Sequences. In: Proc. of ICASSP (2008)
6. Goceri, E.: Automatic Kidney Segmentation Using Gaussian Mixture Model on MRI Sequences. In: Electrical Power System and Computers, vol. 99, pp. 23–29 (2009)
7. Cuingnet, R., Prevost, R., Lesage, D., Cohen, L.D., Mory, B., Ardon, R.: Automatic detection and segmentation of kidneys in 3D CT images using random forests. In: Ayache, N., Delingette, H., Golland, P., Mori, K. (eds.) MICCAI 2012, Part III. LNCS, vol. 7512, pp. 66–74. Springer, Heidelberg (2012)
8. Mory, B., Somphone, O., Prevost, R., Ardon, R.: Real-Time 3D Image Segmentation by User-Constrained Template Deformation. In: Ayache, N., Delingette, H., Golland, P., Mori, K. (eds.) MICCAI 2012, Part I. LNCS, vol. 7510, pp. 561–568. Springer, Heidelberg (2012)
9. Khalifa, F., Elnakib, A., Beache, G.M., Gimel'farb, G., El-Ghar, M.A., Ouseph, R., Sokhadze, G., Manning, S., McClure, P., El-Baz, A.: 3D Kidney Segmentation from CT Images Using a Level Set Approach Guided by a Novel Stochastic Speed Function. In: Fichtinger, G., Martel, A., Peters, T. (eds.) MICCAI 2011, Part III. LNCS, vol. 6893, pp. 587–594. Springer, Heidelberg (2011)
10. Yuksel, S.E., El-Baz, A., Farag, A.A.: A Kidney Segmentation Framework for Dynamic Contrast Enhanced Magnetic Resonance Imaging. J. of Vibr. and Con. 12(9-10), 1505–1516 (2007)
11. Spiegel, M., Hahn, D., Daum, V., Wasza, J., Hornegger, J.: Segmentation of Kidneys using A New Active Shape Model Generation Technique based on Non-Rigid Image Registration. In: Comput. Med. Imaging Graph, vol. 33(1), pp. 29–39 (2009)
12. Zhu, S.C., Yullie, A.: Region Competition: Unifying Snakes, Region Growing, and Bayes/MDL for Multiband Image Segmentation. IEEE Trans. on PAMI, 884–900 (1996)
13. Matas, J., Chum, O., Urban, M., Pajdla, T.: Robust Wide Baseline Stereo from Maximally Stable Extremal Regions. In: Proc. of BMVC, pp. 384–396 (2002)
14. Saranathan, M., Rettmann, D.W., Hargreaves, B.A., Clarke, S.E., Vasanawala, S.S.: Differential Subsampling with Cartesian Ordering (DISCO): A High Spatio-Temporal Resolution Dixon Imaging Sequence for Multiphasic Contrast Enhanced Abdominal Imaging. J. Magn. Reson. Imaging 35(6), 1484–1492 (2012)
15. Otsu, N.: A Threshold Selection Method from Gray-Level Histograms. IEEE Trans. Sys. Man. Cyber 9(1), 62–66 (1979)